

LEVITATION MELTING OF ZIRCONIUM-NIOBIUM ALLOYS AND THEIR STUDY

BY
UMESH CHANDRA SAXENA



PARTMENT OF METALLURGICAL ENGINEERING
INDIAN INSTITUTE OF TECHNOLOGY KANPUR
MAY, 1968

ME
1968
M
SAX
LEV
TH
ME/1968/M
SA 972

CENTRAL LIBRARY
Indian Institute of Technology
KANPUR

Class No 669.735
Sa 97l

Accession No

LEVITATION MELTING OF ZIRCONIUM-NIOBIUM ALLOYS
AND THEIR STUDY

A thesis submitted
In Partial Fulfilment of the requirements
for the Degree of
Master of Technology

by
Umesh Chandra Saxena

to the
Department of Metallurgical Engineering
Indian Institute of Technology, Kanpur

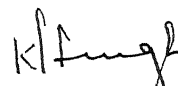
May 1968

ME-1968-M-SAX-LEV

Thesis
669735
Sa 97 L

CERTIFICATE

Certified that the work presented in this thesis
has been carried out by U. C. Saxena under my supervision
and has not been submitted elsewhere for a degree.



Dr. K. P. Singh
Associate Professor
Department of Metallurgical Engineering
I.I.T. Kanpur

ACKNOWLEDGEMENT

The author expresses his deep gratitude to Dr. K. P. Singh who acted as thesis supervisor, for his able guidance, lively interest in the work and fruitful suggestions.

The suggestions and help by Mr. V.K.Sinha are gratefully acknowledged.

Thanks are also due to Mr. S.Krishnamurti for his help and cooperation.

The author also gratefully acknowledges the Department of Atomic Energy, Government of India, for the award of a Research Fellowship and financial assistance during the period of this work.

U. C. Saxena

TABLE OF CONTENTSChapter

	List of Tables	v
	List of Figures	vi
	Synopsis	viii
I	Introduction	1
II	Theory of Levitation Melting	10
III	Experimental Set Up	16
IV	Experimental Procedure	21
V	Study of Alloys	23
VI	Discussion	50
VII	Conclusion	56
	Appendix A	59
	Appendix B	60

LIST OF TABLES

Table 1	Composition of the alloys
Table 2	Microhardness of crystal bar Zirconium
Table 3	Microhardness of Zr-2.5 Wt% Nb obtained from D.A.E. in as cast condition
Table 4	Microhardness of Zr-2.5 Wt% Nb prepared by levitation melting in as cast condition
Table 5	Microhardness of Zr-2.5 Wt% Nb-0.1 Wt% V in as cast condition
Table 6	Microhardness of Zr-2.5 Wt% Nb-0.2 Wt% V in as cast condition
Table 7	Microhardness of Zr-2.5 Wt% Nb-0.3 Wt% V in as cast condition
Table 8	Microhardness of Zr-2.5 Wt% Nb-0.4 Wt% V in as cast condition
Table 9	Microhardness of Zr-2.5 Wt% Nb-0.1 Wt% Ti in as cast condition
Table 10	Microhardness of Zr-2.5 Wt% Nb-0.2 Wt% Ti in as cast condition
Table 11	Microhardness of Zr-2.5 Wt% Nb-0.3 Wt% Ti in as cast condition
Table 12	Microhardness of Zr-2.5 Wt% Nb-0.4 Wt% Ti in as cast condition.

LIST OF FIGURES

- Figure 1 Basic Electric Circuit for levitation melting
- Figure 2 Distribution of induced field
- Figure 3 Levitation chamber
- Figure 4 Levitation coil
- Figure 5 Crystal bar Zirconium-structure
- Figure 6 Zr-2.5 Wt% Nb alloy obtained from the D.A.E.
-structure
- Figure 7 Zr-2.5 Wt% Nb alloy levitation melted
structure in middle
- Figure 8 Zr-2.5 Wt% Nb alloy levitation melted
structure at edges
- Figure 9 Zr-2.5 Wt% Nb-0.1 Wt% V alloy
structure in middle
- Figure 10 Zr-2.5 Wt% Nb-0.1 Wt% V alloy
structure at edges
- Figure 11 Zr-2.5 Wt% Nb-0.2 Wt% V alloy
structure in middle
- Figure 12 Zr-2.5 Wt% Nb-0.2 Wt% V alloy
structure at edges
- Figure 13 Zr-2.5 Wt% Nb-0.3 Wt% V alloy
structure in middle
- Figure 14 Zr-2.5 Wt% Nb-0.3 Wt% V alloy
structure at edges
- Figure 15 Zr-2.5 Wt% Nb-0.4 Wt% V alloy
structure in middle

Figure 16	Zr-2.5 Wt% Nb-0.4 Wt% V structure at edges
Figure 17	Zr-2.5 Wt% Nb-0.1 Wt% Ti structure in middle
Figure 18	Zr-2.5 Wt% Nb-0.1 Wt% Ti structure at edges
Figure 19	Zr-2.5 Wt% Nb-0.2 Wt% Ti structure in middle
Figure 20	Zr-2.5 Wt% Nb-0.2 Wt% Ti structure at edges
Figure 21	Zr-2.5 Wt% Nb-0.3 Wt% Ti structure in middle
Figure 22	Zr-2.5 Wt% Nb-0.3 Wt% Ti structure at edges
Figure 23	Zr-2.5 Wt% Nb-0.4 Wt% Ti alloy structure in middle
Figure 24	Zr-2.5 Wt% Nb-0.4 Wt% Ti alloy structure at edges
Figure 25	The Equilibrium Phase Diagram of Zr-Nb

SYNOPSISLEVITATION MELTING OF ZIRCONIUM-NIOBIUM ALLOYS
AND THEIR STUDY

A thesis submitted
In Partial Fulfilment of the requirements
for the Degree of
Master of Technology

by
Umesh Chandra Saxena

to the
Department of Metallurgical Engineering
Indian Institute of Technology, Kanpur
May 1968

The present work consists of developing a coil for levitation melting of Zirconium and Zirconium-Niobium alloys. The effect of change of coil parameters and melting atmosphere on levitation melting is studied. The work also includes a preliminary study by Metallography and by hardness testing of the alloys made by levitation melting of Zirconium and Niobium with minute additions of Vanadium and Titanium.

CHAPTER - I

INTRODUCTION

Zirconium - 2.5 wt% Niobium is one of the alloys that is of potential interest for fuel element cladding and pressure tubes in water cooled nuclear reactors. Due to its very low thermal neutron absorption cross-section, its high corrosion resistance, and high resistance for irradiation damage, the alloy has become more and more important in recent years. During the early Zirconium alloy studies in the United States Nuclear Programme, the potential of Zirconium-Niobium alloy was partially recognised¹. However Russian investigators reported for the first time at the Second Geneva Conference on the peaceful uses of atomic energy in 1958 that they had been studying in some detail crystal bar Zirconium alloyed with Niobium, and in fact have selected a 2.5 wt% Niobium alloy for actual reactor service².

Till 1958, Zircaloy-2 (Appendix A) was almost universally used as a construction material for pressure tube in atomic reactors. Since the Second Geneva Conference Zirconium alloys with Niobium has been the object of numerous investigations. A number of laboratories in the United States,³ Canada,⁴ England,⁵ Germany^{6,7} have been working with various aspects of the Metallurgy and corrosion behaviour of Zirconium-Niobium alloys.

Unlike Zircaloy-2 and other related alloys, Zirconium-2.5 wt% Niobium can be substantially strengthened by heat treatment. J.K.Dawson et al⁸ advocates strongly for the use of Zirconium-2.5 wt% Niobium for pressure tubes. He mentions that as this alloy has strength 50% higher than Zircaloy-2⁹, the thickness of the pressure tube can be reduced and thus it is possible to achieve neutron economy in the reactors. Apart from having higher mechanical strength, Zirconium-2.5 wt% Niobium alloy has creep strength higher by 50% as compared to Zircaloy-2. The impact strength of Zirconium-2.5 wt% Niobium alloy is better than Zircaloy-2. The suitability of this binary alloy for atomic reactor is further increased as this alloy undergoes a less deleterious effect on tensile strength from neutron irradiation. In addition the impact properties of Zirconium-2.5 wt% Niobium alloy remain superior or equal to those of Zircaloy-2 after equivalent combination of hydrogen addition and irradiation¹⁰. However in water and steam over the temperature range of 400°C the corrosion resistance of the heat treated binary alloy is generally less than that of Zircaloy-2.

ZIRCONIUM-NIOBIUM SYSTEM

The phase diagram of Zirconium-Niobium system has been established by incipient melting tests, thermoresistometric and dilatometric measurements, and X-ray work on quenched alloys by Rogers and Atkins¹¹. The alloys were melted in Tungston

electrode copper-crucible arc furnace in an Argon atmosphere. Because of the sluggishness of the solid state reaction shown by all alloys containing more than 5 Wt% Niobium, the diagram is based on data taken with rising temperatures. The salient features of the diagram being:

1. Complete mutual solid solubility exists for an interval below the solidus line, a continuous curve with a flat minimum near 22% Niobium at 1740°C.

2. The eutectoid horizontal occurs at 610°C and at 17.5% Niobium. It extends from 6.5% to 80% Niobium.

Constitutional work on this system has also been done by Stelton¹², Simcoe and Mudge¹³ and Hodge¹⁴. According to Simcoe and Mudge¹³ less than 0.5 Wt% Niobium is soluble in Zirconium at eutectoid horizontal temperature of 800°C. Hodge¹⁴ investigated the Zirconium-Niobium system upto about 25% Niobium. He suggested eutectoid reaction to occur at 625°C and solubility of Niobium in Zirconium at 625°C to be nearly 6%. Domagala and Mcpherson¹⁵ examined several alloys containing upto 50 Wt% Niobium metallographically in the as cast condition as well as annealed at and quenched from temperatures in the range 600 - 1600°C. They found the eutectoid reaction to occur at 800°C about 200°C higher than suggested by Rogers and Atkins¹¹ and solubility of Niobium in Zirconium to be less than 5 Wt%.

Richter et al¹⁶ established that oxygen content of the alloys leads to a distinct ternary character of the phase diagram. In this way the eutectoid point of the binary system is extended over a transformation range, which in the case of alloys made from iodide Zirconium is about 100°C and in case of alloys made from sponge Zirconium is over 200°C. They placed the solubility of Niobium in α -Zirconium about 2 Wt%, actual value being sensitive to the purity of original material specially with respect to Oxygen content. Bichkov et al¹⁷, using dilatometric technique placed the eutectoid temperature at 560°C with a Niobium content of 12%. Investigations by Knapton¹⁸, who used chiefly Metallographic technique suggested the solubility of Niobium to be less than 1 at.% in α -Zirconium at the eutectoid temperature of 610°C. Lundin et al¹⁹ studied the whole range of Zirconium-Niobium alloys and established the equilibrium diagram as seen in Appendix B. According to Lundin solubility limit of Niobium in α -Zirconium is 0.1%.

MELTING TECHNIQUE

In making of Zirconium alloys with Niobium a number of difficulties are encountered. Zirconium imposes several severe handicaps on the melter of the more common metals. At its melting point of 1860°C, it attacks all known refractories and is commonly said to be a "Universal Solvent" where crucible materials are concerned. In addition, its extreme affinity for

Oxygen and Nitrogen makes melting in the absence of air mandatory. Both Oxygen and Nitrogen embrittles the metal; Zirconium containing over 2000 ppm of Oxygen being too hard to cold work²⁰. In addition, Nitrogen seriously impairs the corrosion resistance to hot water.

Vacuum Induction Melting

The search for suitable refractory material and melting technique has been wide spread. A study of vacuum induction melting of Zirconium and some of its alloys was made by H.A. Saller, R.F. Dickerson and E.L. Foster, Jr.²¹. It was appreciated by the investigators that vacuum-induction melting in graphite crucibles resulted in contamination, which reduced the corrosion resistance of the metal. Despite this failing it was considered that the case of melting various materials ranging from sponge to scrap made the technique worthy of study. Operating pressures were of the order 1×10^{-3} mm of mercury. The following conclusions were made:

1. Induction melting of sponge Zirconium can be carried out without the special preparations needed for arc melting, thus reducing the ultimate cost of the finished product.

2. Induction melted sponge Zirconium and its alloys have higher tensile strengths and correspondingly higher hardness than similar arc-melted material but are considerably less ductile.

3. Induction melted Zircaloy-2 is more resistant to corrosion than either a 2.5 or a 5% induction melted tin alloys,

but it does not compare on corrosion resistance with a corresponding arc melted alloy .

It can be finally concluded that induction melted Zirconium can not be used as direct substitute for arc-melted material for all purposes and especially for atomic reactor applications, where the material has to meet severe restrictions set by operating conditions.

Arc Melting

A very successful method for melting high melting point reactive metals like Zirconium and its alloys without contamination is the electric arc technique operating in vacuum or in an atmosphere of pure Argon with water cooled copper crucible. This method was used originally in 1903 by Von Bolton to melt Tantalum and appears to have excited little interest until W.J.Kroll²² resurrected in 1940. The method was subsequently developed by the Battelle Memorial Institute where it was used to melt Titanium and its alloys on a small scale²³. While it is possible by this method to build up ingots of metal free from crucible contamination, it is difficult to ensure homogeneity as the sponge tends to vary slightly in composition²⁴.

Levitation Melting

A novel method of melting metals without crucible has been developed recently. The technique is popularly known as Levitation Melting.

Levitation of a solid or molten conductor by means of an electro-magnetic field on theoretical basis was first suggested 45 years ago by Muck²⁵, but apparently not put into practice. Some twenty years later, Lovel²⁶ proposed electro-magnetic levitation without melting. The scope of the technique was first investigated in the laboratories of Westinghouse Electric Corporation by Okress²⁷⁻²⁹ et al in seeking a means of melting more reactive metals of high melting points, such as Ti, Zr, V, Ta, Mo without contamination from crucible material.

Levitation melting on a scale of 5 to 8 gm., for variety of metals in an inert atmosphere by the employment of 400 Kc was first described by Polonis et al^{30,31}. Their work demonstrated the usefulness of the method as a small scale laboratory melting technique. Interest in the new melting technique is reflected in several review articles by Braunbek³², Winkler³³, Schiebe³⁴ and in a popular periodical³⁵.

Inherent advantages of Levitation melting have been responsible for continued development, on a laboratory scale. The more important advantages are:

1. Non contamination of melt - an important advantage, and early recognised as such for reactive metals^{27,34,36} and more recently for physico chemical studies of gas-liquid metal system; in the past later presented difficulties in interpretation due to possible side reactions with crucible materials.

2. Homogeneity of melt due to very efficient stirring- homogeneity is also retained in the ingot due to rapidity of solidification as noted by Polonis^{30,37}. Comenetz and Salatka obtained greater homogeneity than was obtainable by repeated arc melting^{38,39}. Peifer⁴⁰ obtained improved uniformity in the gas contents of samples of ferro-alloys.

3. Rapid attainment of equilibrium in gas-liquid metal systems - due to the relatively large surfaces exposed to the gas phase, and to efficient stirring. The rate is further enhanced when the gas flows past the molten sphere. In this manner, Peifer⁴⁰ was able to increase the nitrogen content of molten pure iron from 2 ppm to the equilibrium solubility level of 445 ppm in 50 sec.

4. Fine dispersion - in alloys where two or more phases separate out during solidification, the fast cooling rate available ensures fine dispersion.

The chief disadvantage results from difficulties of temperature control and its measurement.

A lesser disadvantage is the relatively severe vapourization of high vapour pressure elements due to large surface to volume and rapid stirring.

Weight of molten charge is also limited to few grams.

Low electrical efficiency and occasional instability of molten charge are also minor problems.

STATEMENT OF PROBLEM

In view of extremely high melting point of Zirconium (1860°C) and Niobium (2468°C) and its attacking power to all known refractories in conjunction with the promising feature of Levitation Melting technique it was proposed to melt Zirconium and make its alloys with Niobium with very minor additions of Titanium and Vanadium in a crucibleless manner in an inert atmosphere. It was also proposed to make a preliminary study of alloys thus made metallographically and by hardness testing.

CHAPTER - II

THEORY OF LEVITATION MELTING

ELECTRO-MAGNETIC FIELD FOR LEVITATION

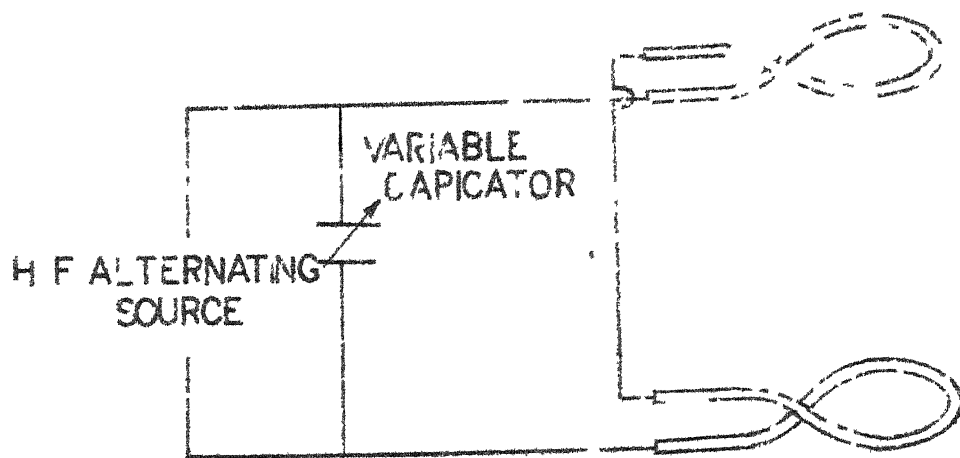
A conductor placed in an electro-magnetic field will move from the stronger to the weaker part of the field. For levitation, the field strength must decrease vertically to provide a lifting force equal to the weight of the conductor. For lateral stability, the field must decrease radially towards the field axis, thus providing a restoring force towards the axis.

Such a field is obtained from two coaxial coils matched to a high frequency generator. As shown schematically in Fig.1, a variable capacitance will provide the means of tuning the load to the generator for maximum power transfer to the coils. The coils in practice are generally unequal and carry alternate current with a 180° phase difference.

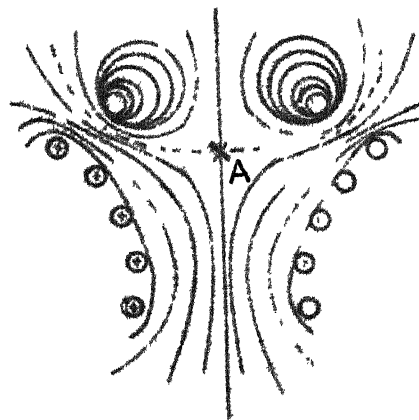
Fig.2 shows a field and coil configuration suitable for levitation as reported by Jenkins et al⁴¹. In Fig.2, point A is the position of minimum field strength, so that a conductor placed in this field will experience a force tending to move it towards point A. Weightless conductor would remain at this point. In practice, an equilibrium of field and gravitational force will determine the final position of the conductor to be somewhat below point A.

LEVITATION MELTING UNIT

TUNED CIRCUIT



BASIC ELECTRIC CIRCUIT FOR LEVITATION MELTING
FIG. 1



DISTRIBUTION OF INDUCED FIELD
FIG 2

LEVITATION FORCE

The fundamental equations of levitation theory were first stated by Okress et al²⁷, in which a complex quantitative relationship was given for the important factors determining the levitating force on a solid sphere. The fundamental result of their calculations is that the metal sphere behaves as an idealized dipole loop. They experimentally demonstrated that their theoretical result for the levitating force is accurate for a 1 inch bronze ball suspended between two coaxial loops with current flowing in reverse directions as shown in Fig.1. For 1.5 inch ball the measured value was only 5/6th of the calculated value.

The derived relationship of Okress et al²⁷, indicates the levitation force is directly proportional to the square of the coil current and to a complex function of a parameter X. Since parameter X is proportional to the square root of the frequency, the higher the frequency the larger the value of X. $G(X)$ function increases asymptotically with X. X is also inversely proportional to the square root of electrical resistivity.

The relation is

$$F = \frac{3}{50} \pi^2 I^2 G(X) A(Y) \left(\frac{R_2}{R_1} \right)^3$$

where

F = Force in dynes

I = Amplitude of alternating current in R.M.S.amp.

R_2 = Radius of sphere

R_1 = Radius of coil

$$X = 2 \pi R_2 \left(\frac{\nu}{\rho \times 1000} \right)^{\frac{1}{2}}$$

$$G(X) = 1 - \frac{3 \sinh 2X - \sin 2X}{4X \sinh^2 X + \sin^2 X}$$

$$Y = \frac{2}{R_1}$$

$$A(Y) = \frac{Y}{(1+Y^2)^4}$$

ν = Frequency of alternating current in cycles/sec.

ρ = Resistivity of spherical charge

However this relation is valid only for cylindrical coil and spherical charge.

TEMPERATURE CONTROL

The steady state temperature of a levitated charge depends upon the properties of the charge material, characteristic of the levitation system and the heat dissipated by the charge. Materials of greater mass or density and higher electrical resistivity levitate lower in the coil where the field strength is greater and thus heated to greater extent. Decreasing the power also permits the charge to drop lower into the coil with same effect on temperature.

Temperature control of the levitated charge has probably been the area of greatest difficulty in developing the levitation

melting technique. The difficulty is inherent in the electrical equipment as currently designed, which requires that both the levitation force and heating of the metal must be controlled, by the current control of the induction heater. Thus high field strength required to support a high density material also often results in higher than desired temperature.

However, in the present case where aim was to develop levitation technique for melting and alloying only, temperature control was not a problem. But where some studies have to be made on liquid levitated metal, temperature control may be a limitation to the technique.

However, an alternative method of temperature control has been suggested⁴⁰. A separate method of cooling charge by static or dynamic gaseous atmosphere can be used to advantage for temperature control. Cooling can be affected by flowing gases of different thermal conductivity over the levitated metal. As radiation losses depend upon the pressure of the gas, the pressure of gas may form a basis for temperature control. Also radiation losses depend upon conductivity of gases, mixture of gases can be used for temperature control.

TEMPERATURE MEASUREMENT

Measuring the temperature of levitated metal presents difficulty. Thermocouples are not conveniently used or even undesirable because of possible melt contamination, and in

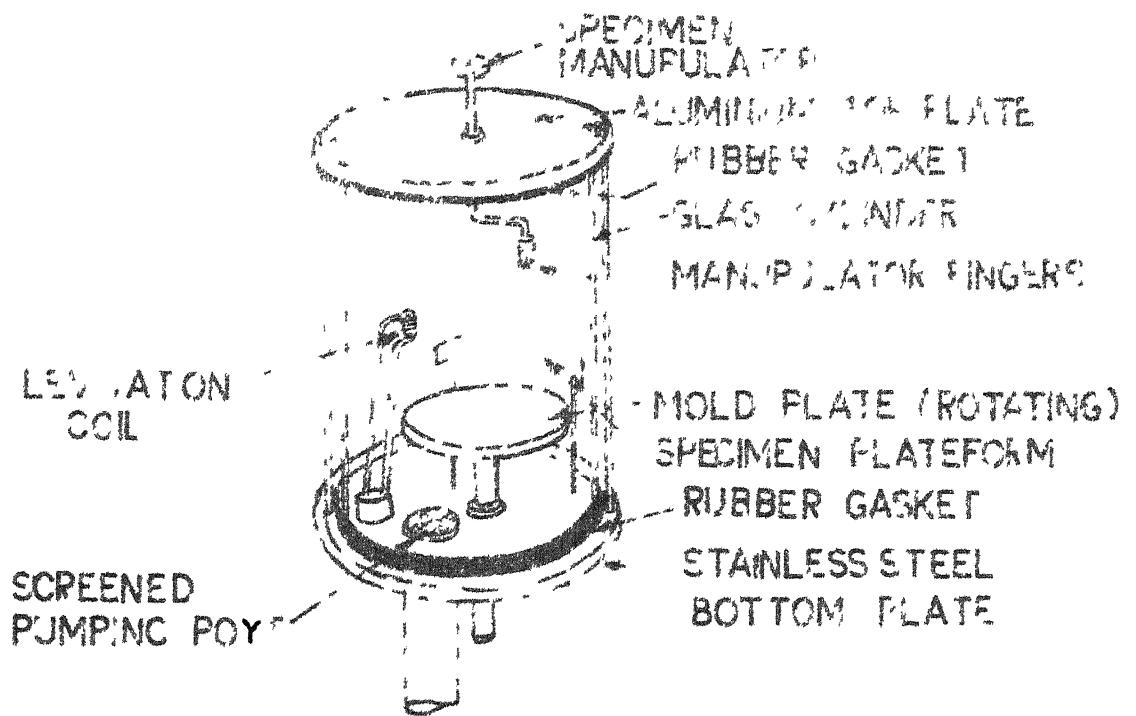
many cases the temperature is too high. These objections do not apply to the optical pyrometer, but another difficulty does arise due to the non-black body conditions associated with an unenclosed body. Temperatures can not be measured with accuracy without prior knowledge of emissivity. If, however, the emissivity is known, the temperature can be determined with good accuracy by means of an optical pyrometer.

In the present case because of these difficulties and also because it was not essential, no attempt to measure temperature was made.

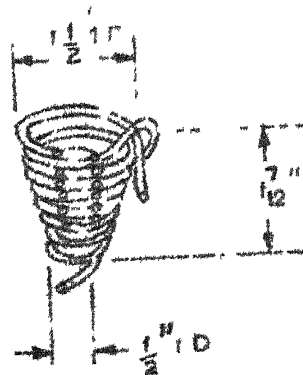
CHAPTER - III

EXPERIMENTAL SET UPLEVITATION CHAMBER

A schematic diagram of levitation chamber is shown in Fig.3. The chamber consisted of a stainless steel plate over which a pyrex bell was placed, the junction being sealed by neoprene gasket. The top of the chamber was covered by a aluminium plate again sealed with neoprene gasket. The system was connected to ^{or} diffusion pump backed by mechanical pump. Vacuum was measured ^{by} ~~in~~ cold cathod gauge or thermocouple gauge depending upon the order of vacuum. When diffusion pump is conjunction with mechanical pump, the vacuum obtained was 5×10^{-2} microns. The vacuum obtained with mechanical pump was 10 microns. It was thought convenient to operate only with mechanical pump as system was flushed two-three times with Argon. Inert gas was maintained through the needle valve. Inside the levitation chamber there was a specimen manipulator which held the specimen and when pressed dropped the specimen into the copper coil. There was a specimen platform on which various specimen to be melted could be kept. Copper molds were kept on the copper disc which could be rotated to the desired position. The levitation coil was introduced in the coil was introduced in the chamber through Neoprene rubber cork fitted in the bottom plate of the levitation chamber and was connected to high tension leads coming from power source. Inside the chamber a cylindrical Aluminium net was placed



TO DIFFUSION PUMP
BACKED BY A MECHANICAL PUMP
LEVITATION CHAMBER
FIG. 3



COIL
FIG. 4

to shield the radiations from inside to outside the chamber.

ARGON

Pure Argon was prepared by passing commercial cylinder Argon through the beds of copper turnings and Titanium granules maintained at 550°C and 850°C respectively in the furnaces.

POWER SOURCE

High frequency power was taken from Ajax Magnethermic radio frequency generator. The r-f generator consisted of a rectifier and an oscillator. The rectifier converted the 50 cycles power frequency to high voltage d-c power, and the oscillator converted the high voltage d-c power to r-f power.

The components of the unit were housed in a steel cabinet divided into three compartments; namely, the oscillator, rectifier compartment and the control compartment. Access was obtained through the rear panels to the rectifier compartment, the large door and side panel to the oscillator compartment, and small door to the control compartment.

The power supply was 3 phase 400 volts at 50 cycles. The output of the generator was 20 KW at 450 Kc.

All operational adjustments to the machine were made from the outside of the unit. The operational controls, meters, and check lights which indicated the performance of the

equipment were located on the front panel. Plate voltage and plate current indicated by the meters were controlled by a power control knob. Grid current was adjusted by grid control knob. Any irregularity or fault in the operation was indicated by various check lights.

LEVITATION COIL

The design of the levitation coil has been mostly empirical. However, now certain guide lines for designing are available eg. levitating force increases with the number of turns of the coil, smaller dia coil provide higher field strength etc.

As levitating force increases with increase in number of turns per unit length. $1/8$ " O.D. copper tube, the smallest dia tube which can be water cooled sufficiently was used. Though various workers have suggested various coil designs, the conical type of coils were found to be more promising. The coils with varying apex semiangle starting from 15° , 20° , 30° , 40° and 60° were tried. The coil with apex semiangle of 30° was found to be most suitable for Zirconium levitation. Also several coils with varying number of turns were investigated. Out of all the trials and errors, the coil found most successful for levitation of Zirconium is given in Fig.4. The coil is in a form of a cone with apex downward and topmost turn wound in reverse direction. The bottommost turn is $\frac{1}{2}$ " dia

and uppermost turn is of $1\frac{1}{2}$ " dia, the vertical height between the coil is $1\frac{7}{12}$ " with total of 7 direct and 1 reverse turn. The coil semiangle is of 30° .

The levitation coil is cooled by flowing water through it in order to protect it from damage from the molten charge inside it. Flow rate of water was kept at 0.4 litres/minute.

CHAPTER - IV

EXPERIMENTAL PROCEDURE

The metal to be melted was machined to a cylindrical shape. The size of the specimen was found to be very critical and was arrived at by trials and errors. The optimum size was found to be such that it just touched the bottommost coil turn when placed over it. For continuous melting, various such specimen were placed on specimen plateform and with the help of manipulator dropped in the coil. For alloy preparation, the alloying element was placed over the specimen which had been previously dropped into the coil.

Whole system was evacuated with the help of mechanical pump after placing the specimen in the coil. When the system attained vacuum of about 10 microns, the chamber was flushed with purified Argon two to three times and reevacuated and finally filled with purified Argon at 1 atm. pressure. Cooling water was kept flowing through the coil at the rate of 0.4 litres/minute.

In the last power was turned on. With the control knob internally connected to variable capacitance, the load was tuned to the circuit. For maximum coupling i.e. for maximum power transfer to the coil, the ratio between grid current to plate current was maintained between 6 - 10. Plate voltage was

raised gradually till the specimen levitate melted. In general, melting is complete within 15 - 20 seconds. After melting it whirled and remain levitated for few seconds. When power was reduced the melt dripped down in the mold kept down the coil. For another melt, the mold table is rotated so that a new mold took the place of previous one and charge was dropped from the specimen manipulator and whole operation was repeated.

In this way following alloys as given in Table 1 were made. The weighing of the specimen was done with micro-metlar balance.

TABLE 1

Alloy Serial No.	Wt. of Zr in gm.	Wt. of Nb in gm.	Wt. of Ti in gm.	Wt. of V in gm.	Nominal Composition
Alloy 1	1.5237	0.0392	-	-	Zr-2.5 Nb.
Alloy 2	1.6384	0.0421	0.0165	-	Zr-2.5 Nb-0.1Ti
Alloy 3	1.6024	0.0406	0.0328	-	Zr-2.5 Nb-0.2Ti
Alloy 4	1.5846	0.0401	0.0475	-	Zr-2.5 Nb-0.3Ti
Alloy 5	1.5492	0.0398	0.0647	-	Zr-2.5 Nb-0.4Ti
Alloy 6	1.8346	0.0458	-	0.0184	Zr-2.5 Nb-0.1V
Alloy 7	1.8675	0.0465	-	0.0371	Zr-2.5 Nb-0.2V
Alloy 8	1.9244	0.0486	-	0.0572	Zr-2.5 Nb-0.3V
Alloy 9	1.9515	0.0492	-	0.0778	Zr-2.5 Nb-0.4V

CHAPTER - V

STUDY OF THE ALLOYS

METALLOGRAPHY

Zirconium and its alloys are difficult to be prepared for microscopic examination due to the tendency of the metal to flow and shear during grinding and polishing. Nevertheless several authors have described various methods.

Generally recommended practice for metallographic revelation is for chemical or electrochemical polishing followed by etching. However in present case it was possible to prepare the specimen for metallographic examination by mechanical polishing i.e. polishing with emery paper, coarse Allumina powder followed by fine Allumina powder on the polishing wheel.

A large number of etchants have been prescribed by various investigators⁴²⁻⁴⁶. All of these reagents contain Hydrofluoric acid and water with and without Glycerine and Nitric acid. The etchant of following composition was found to be quite good to reveal the microstructural details in 20 - 30 seconds. The composition of etchant is:

15 ml HF

35 ml HNO₃

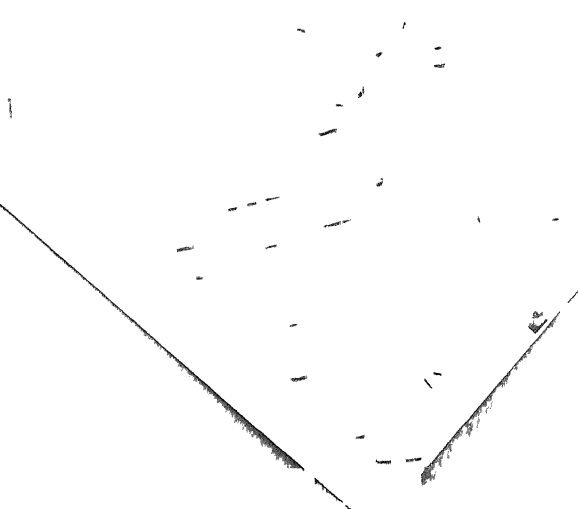
60 ml Distilled water

Fig.5

castal bar Zirconium

Magn. - 100X

enlarged 10 times on enlarger



Zr-2.5 Wt% Nb alloy obtained from D.A.E.

Magn. 400X

Further enlarged 10 times on enlarger

Fig.7

Zr-2.5 Wt% Nb alloy
Structure obtained in middle of the specimen
Magn. 400X
Further enlarged 10 times on enlarger

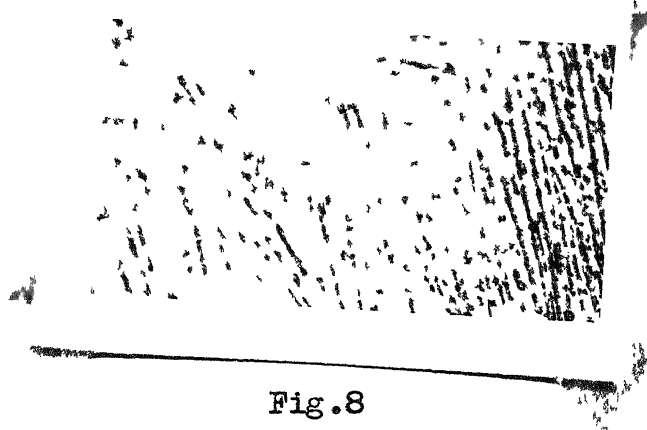


Fig.8

Zr-2.5 Wt% Nb alloy
Structure obtained at edges of the specimen
Magn. 400X
Further enlarged 10 times on enlarger




Fig.9

Zr-2.5 Wt% Nb-0.1%V

Structure obtained in middle of the specimen

Magn. 400X

Further enlarged 10 times on enlarger



Fig.10

Zr-2.5 Wt% Nb-0.1%V

Structure obtained at edges of the specimen

Magn. 400X

Further enlarged 10 times on enlarger

Fig.11

Zr-2.5 Wt% Nb-0.2 Wt%V

Structure obtained in middle of the specimen

Magn. 400X

Further enlarged 10 times on enlarger

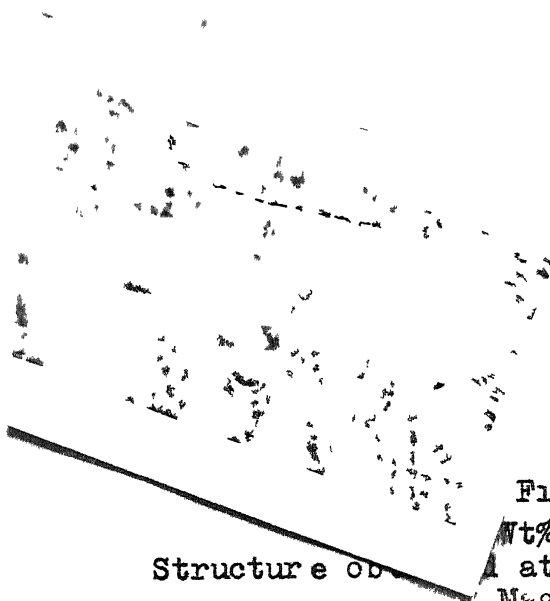


Fig.12

Wt% Nb-0.2 Wt%V

Structure obtained at edges of the specimen

Magn. 400X

Further enlarged 10 times on enlarger

Fig. 13

Zr-2.5 Wt% Nb-0.3 Wt% V
Structure obtained in middle of the specimen
Magn. 400X

Further enlarged 10 times on enlarger

Fig. 14

Zr-2.5 Wt% Nb-0.3 Wt% V
Structure obtained at edges of the specimen
Magn. 400X

Further enlarged 10 times on enlarger

Fig.15

Zr-2.5 Wt% Nb-0.4 Wt% V
Structure obtained in middle of the specimen
Magn.400X
Further enlarged 10 times on enlarger

Fig.16

Zr-2.5 Wt% Nb-0.4 Wt% V
Structure obtained at edges of the specimen
Magn. 400X
Further enlarged 10 times on enlarger



Fig.17

Zr-2.5 Wt% Nb-0.1 Wt% Ti
Structure obtained in middle of the specimen
Magn. 400X
Further enlarged 10 times on enlarger



Fig.18

Zr-2.5 Wt% Nb-0.1 Wt% Ti
Structure obtained at edges of the specimen
Magn. 400X
Further enlarged 10 times on enlarger




Fig.19

Zr-2.5 Wt% Nb-0.2 Wt% Ti
Structure obtained in middle of the specimen
Magn.400X
Further enlarged 10 times on enlarger




Fig.20

Zr-2.5 Wt% Nb-0.2 Wt% Ti
Structure obtained at edges of the specimen
Magn. 400X
Further enlarged 10 times on enlarger

Fig.21

Zr-2.5 Wt% Nb-0.3 Wt% Ti

Structure obtained in middle of the specimen

Magn. 400X

Further enlarged 10 times on enlarger

Fig.22

Zr-2.5 Wt% Nb-0.3 Wt% Ti

Structure obtained at edges of the specimen

Magn. 400X

Further enlarged 10 times on enlarger



Fig.23

Zr-2.5 Wt% Nb-0.4 Wt% Ti
Structure obtained in middle of the specimen
Magn.400X
Further enlarged 10 times on enlarger

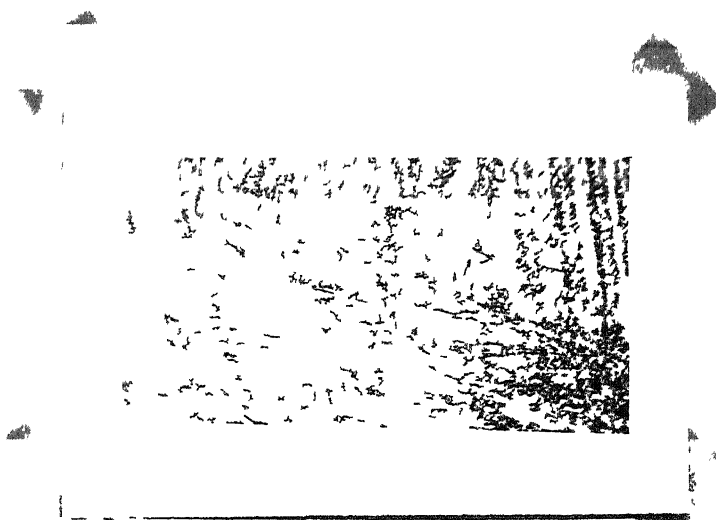


Fig.24

Zr-2.5 Wt% Nb-0.4 Wt% Ti
Structure obtained at edges of the specimen
Magn.400X
Further enlarged 10 times on enlarger

HARDNESS

Microhardness testing of the Zirconium and Zirconium-Niobium alloys were carried by Tukon Microhardness tester. 136° Diamond pyramid indenter was used. Tests were made with 1 kg load. Results are given in Tables 2 - 12. The variation of hardness with distance for the alloys has been plotted in Fig.25 - 34.

TABLE 2
Microhardness of crystal bar Zirconium

S.No.	Distance from edge in mm.	Diamond pyramid hardness number	S.No.	Distance from edge in mm.	Diamond pyramid hardness number
1	0	84	12	5.5 mm	80
2	0.5	86	13	6.0	78
3	1.0	82	14	6.5	82
4	1.5	80	15	7.0	78
5	2.0	84	16	7.5	84
6	2.5	80	17	8.0	80
7	3.0	86	18	8.5	78
8	3.5	84	19	9.0	84
9	4.0	78	20	9.5	80
10	4.5	82	21	10.0	78
11	5.0	88	22	10.5	82
Average Hardness = 82 D.P.H.					

TABLE 3

Microhardness of Zr-2.5 Wt% Nb obtained from D.A.E.
in as cast condition.

S.No.	Distance from edge in mm.	Diamond pyramid hardness number	S.No.	Distance from edge in mm.	Diamond pyramid hardness number
1	0	284	13	6.0	282
2	0.5	287	14	6.5	286
3	1.0	282	15	7.0	291
4	1.5	282	16	7.5	284
5	2.0	286	17	8.0	287
6	2.5	294	18	8.5	291
7	3.0	291	19	9.0	286
8	3.5	287	20	9.5	291
9	4.0	292	21	10.0	284
10	4.5	284	22	10.5	287
11	5.0	291	23	11.0	291
12	5.5	286	24	11.5	286

TABLE 4

Microhardness of Zr-2.5 Wt% Nb prepared by Levitation
melting in as cast condition.

S.No.	Distance from edge in mm.	Diamond pyramid hardness number	S.No.	Distance from edge in mm.	Diamond pyramid hardness number
1	0	373	10	4.5	291
2	0.5	370	11	5.0	286
3	1.0	282	12	5.5	284
4	1.5	287	13	6.0	291
5	2.0	291	14	6.5	292
6	2.5	286	15	7.0	286
7	3.0	282	16	7.5	286
8	3.5	284	17	8.0	368
9	4.0	284	18	8.5	370

TABLE 5

Microhardness of Zr-2.5 Wt% Nb-0.1 Wt% V in
as cast condition.

S.No.	Distance from edge in mm.	Diamond pyramid hardness number	S.No.	Distance from edge in mm.	Diamond pyramid hardness number
1	0	370	11	5.0	294
2	0.5	368	12	5.5	284
3	1.0	287	13	6.0	286
4	1.5	291	14	6.5	282
5	2.0	294	15	7.0	284
6	2.5	286	16	7.5	287
7	3.0	291	17	8.0	287
8	3.5	294	18	8.5	291
9	4.0	287	19	9.0	370
10	4.5	286	20	9.5	373

TABLE 6

Microhardness of Zr-2.5 Wt% Nb-0.2 Wt% V in
as cast condition.

S.No.	Distance from edge in mm.	Diamond pyramid hardness number	S. No.	Distance from edge in mm.	Diamond pyramid hardness number
1	0	370	9	4.0	286
2	0.5	371	10	4.5	287
3	1.0	287	11	5.0	291
4	1.5	291	12	5.5	291
5	2.0	294	13	6.0	294
6	2.5	287	14	6.5	291
7	3.0	296	15	7.0	369
8	3.5	297	16	7.5	370

TABLE 7

Microhardness of Zr-2.5 Wt% Nb-0.3 Wt% V in
as cast condition.

S.No.	Distance from edge in mm.	Diamond pyramid hardness number	S.No.	Distance from edge in mm.	Diamond pyramid hardness number
1	0	369	10	4.5	291
2	0.5	370	11	5.0	294
3	1.0	291	12	5.5	296
4	1.5	296	13	6.0	292
5	2.0	294	14	6.5	291
6	2.5	289	15	7.0	294
7	3.0	292	16	7.5	294
8	3.5	292	17	8.0	370
9	4.0	296	18	8.5	372

TABLE 8

Microhardness of Zr-2.5 Wt% Nb-0.4 Wt% V in
as cast condition.

S.No.	Distance from edge in mm.	Diamond pyramid hardness number	S.No.	Distance from edge in mm.	Diamond pyramid hardness number
1	0	371	11	5.0	299
2	0.5	369	12	5.5	305
3	1.0	303	13	6.0	296
4	1.5	305	14	6.5	296
5	2.0	299	15	7.0	301
6	2.5	299	16	7.5	303
7	3.0	297	17	8.0	301
8	3.5	301	18	8.5	297
9	4.0	301	19	9.0	370
10	4.5	297	20	9.5	371

TABLE 9

Microhardness of Zr-2.5 Wt% Nb-0.1 Wt% Ti in
as cast condition.

S.No.	Distance from edge in mm.	Diamond pyramid hardness number	S.No.	Distance from edge in mm.	Diamond pyramid hardness number
1	0	370	12	5.5	286
2	0.5	371	13	6.0	283
3	1.0	291	14	6.5	291
4	1.5	294	15	7.0	291
5	2.0	286	16	7.5	287
6	2.5	291	17	8.0	294
7	3.0	287	18	8.5	291
8	3.5	287	19	9.0	372
9	4.0	294	20	9.5	374
10	4.5	291			
11	5.0	291			

TABLE 10

Microhardness of Zr-2.5 Wt% Nb-0.2 Wt% Ti in
as cast condition.

S.No.	Distance from edge in mm.	Diamond pyramid hardness number	S.No.	Distance from edge in mm.	Diamond pyramid hardness number
1	0	398	9	4.0	366
2	0.5	396	10	4.5	366
3	1.0	368	11	5.0	370
4	1.5	373	12	5.5	368
5	2.0	373	13	6.0	366
6	2.5	370	14	6.5	368
7	3.0	368	15	7.0	398
8	3.5	368	16	7.5	399

TABLE 11

Microhardness of Zr-2.5 Wt% Nb-0.3 Wt% Ti
in as cast condition.

S.No.	Distance from edge in mm	Diamond pyramid hardness number	S.No.	Distance from edge in mm.	Diamond pyramid hardness number
1	0	402	10	4.5	375
2	0.5	399	11	5.0	373
3	1.0	373	12	5.5	370
4	1.5	373	13	6.0	368
5	2.0	370	14	6.5	375
6	2.5	368	15	7.0	370
7	3.0	370	16	7.5	373
8	3.5	373	17	8.0	399
9	4.0	375	18	8.5	402

TABLE 12

Microhardness of Zr-2.5 Wt% Nb-0.4 Wt% Ti
in as cast condition.

S.No.	Distance from edge in mm.	Diamond pyramid hardness number	S.No.	Distance from edge in mm.	Diamond pyramid hardness number
1	0	405	13	6.0	375
2	0.5	402	14	6.5	373
3	1.0	373	15	7.0	370
4	1.5	378	16	7.5	373
5	2.0	375	17	8.0	378
6	2.5	370	18	8.5	375
7	3.0	370	19	9.0	402
8	3.5	373	20	9.5	402
9	4.0	373			
10	4.5	375			
11	5.0	375			
12	5.5	378			

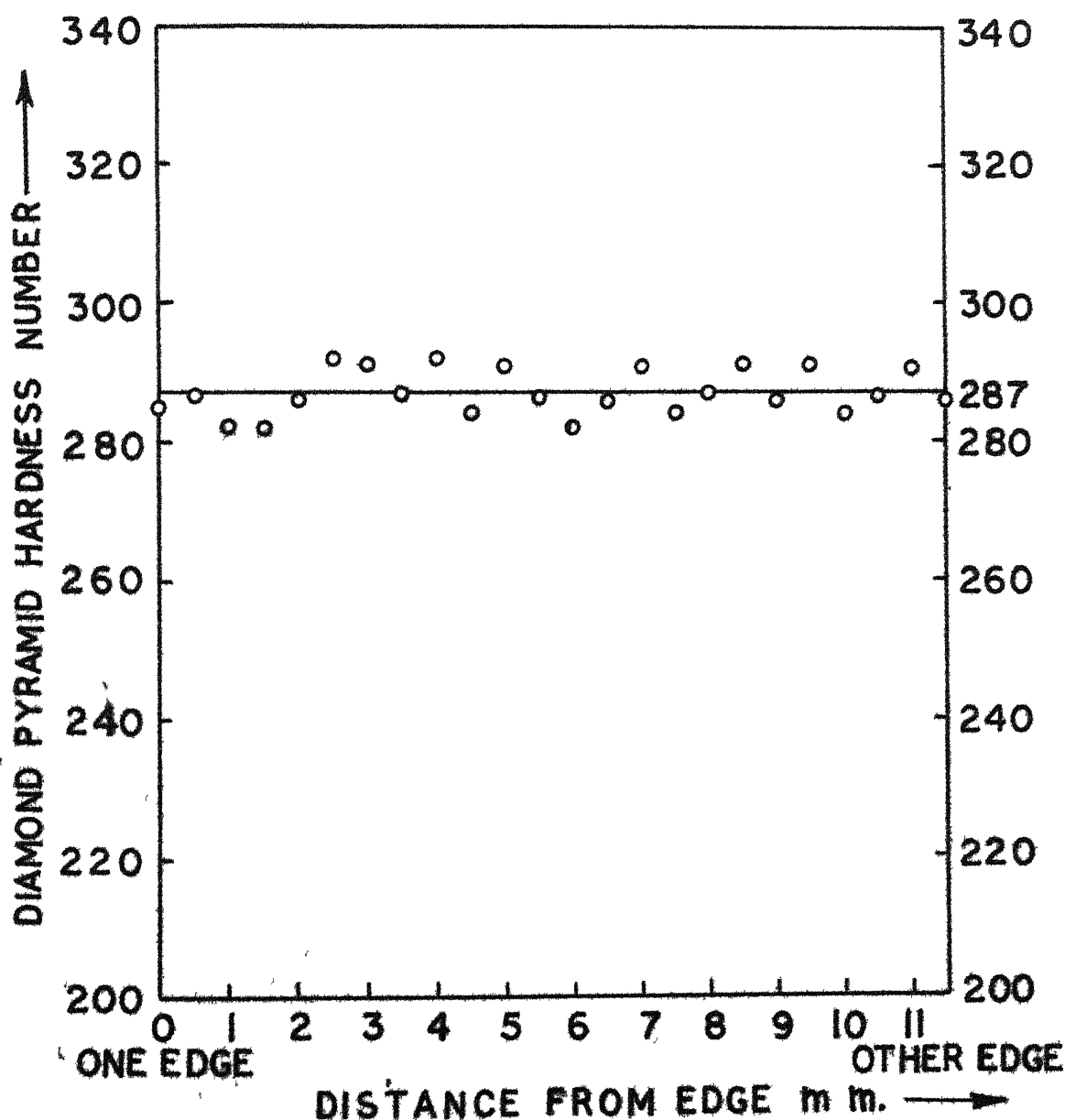


FIG. 25. MICROHARDNESS OF Zr-2.5 Wt % Nb OBTAINED FROM D.A.E IN AS CAST CONDITION.

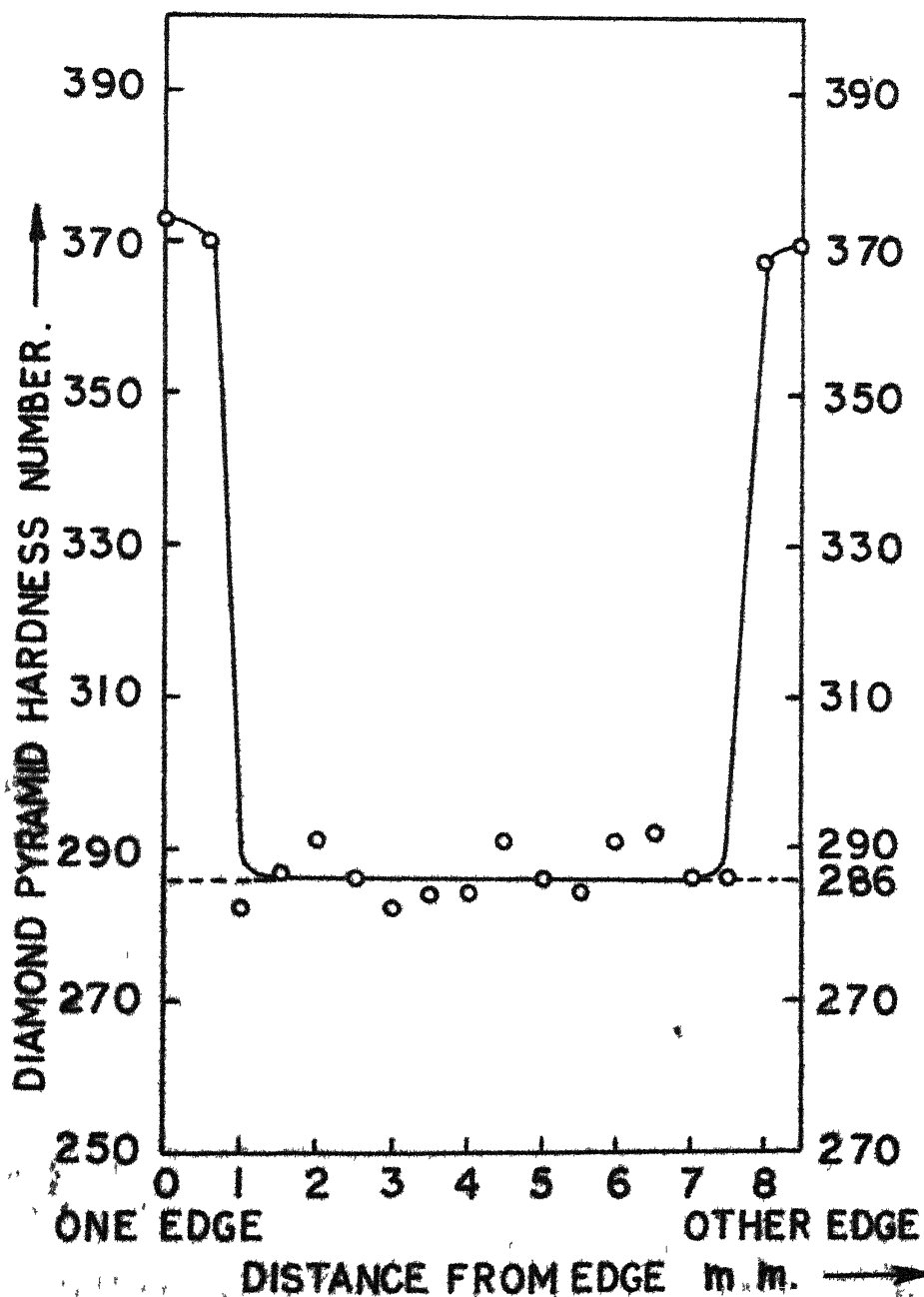


FIG. 26. MICROHARDNESS OF Zr-2.5W-1%Nb
LEVITATION MELTED IN AS CAST
CONDITION.

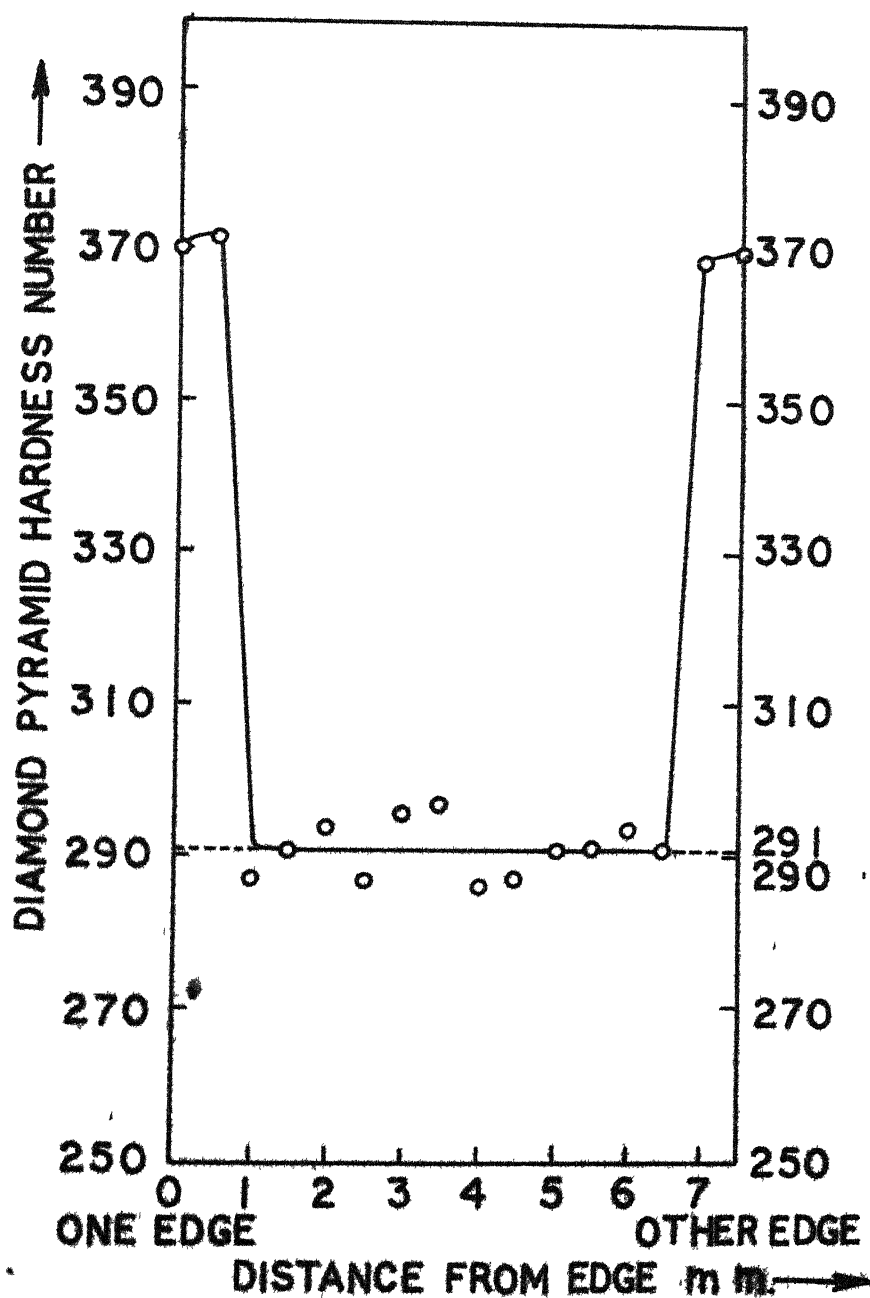
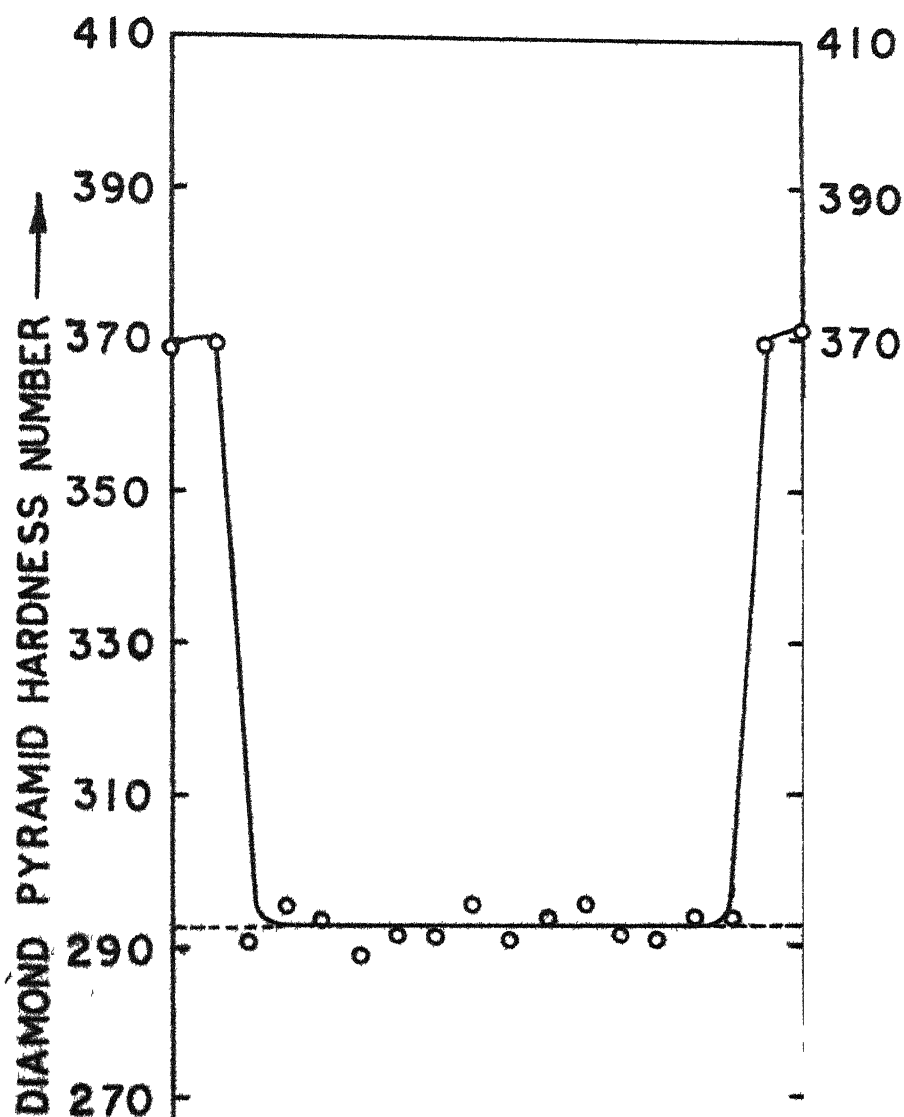


FIG28. MICROHARDNESS OF Zr-2.5Nb-2V
LEVITATION MELTED IN AS CAST
CONDITION.



1 2 3 4 5 6 7 8
DGE OTHE

DISTANCE FROM EDGE m.m.
9. MICROHARDNESS OF Zr-2.5%
LEVITATION MELTED IN AS C
CONDITION

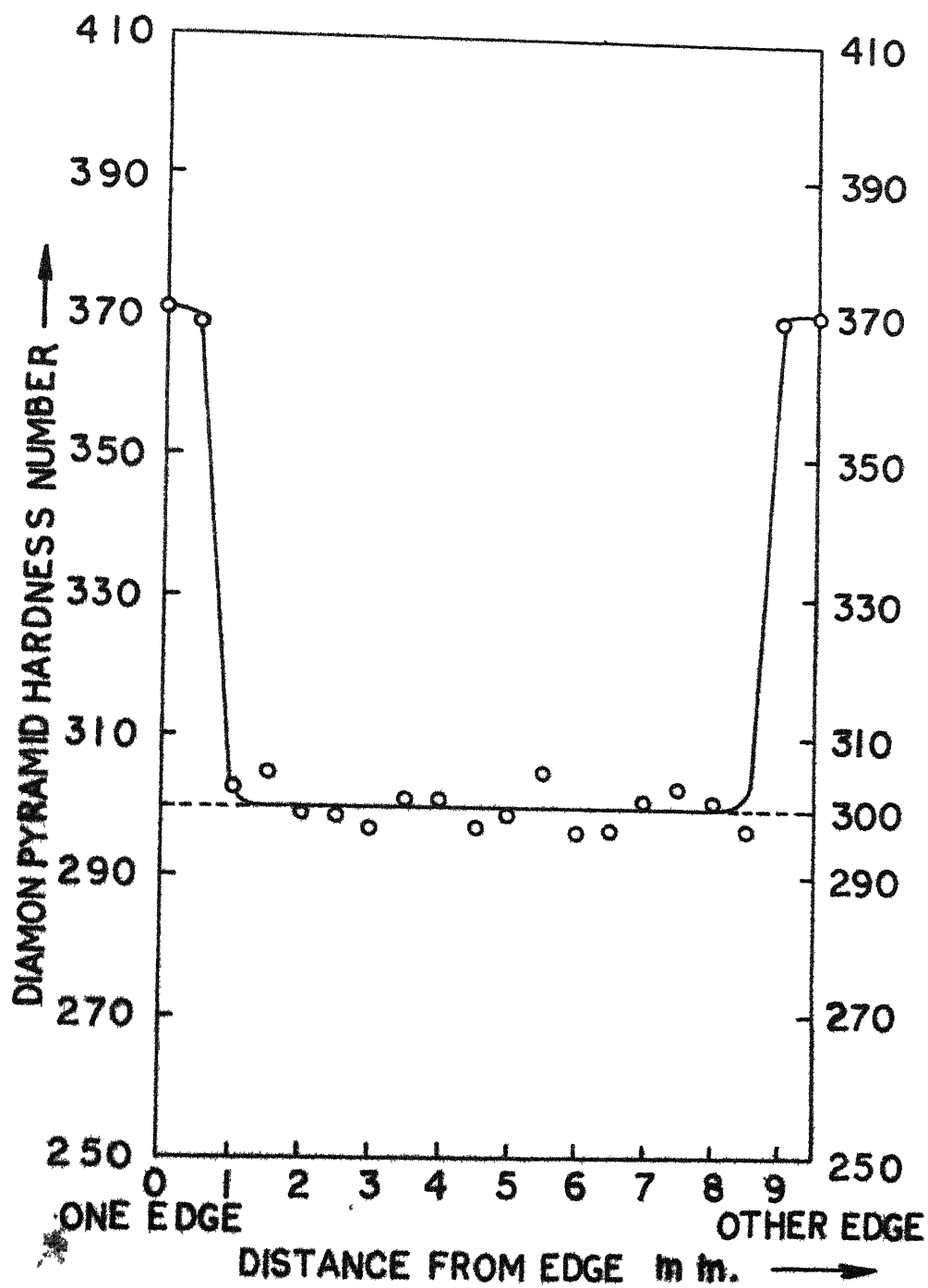
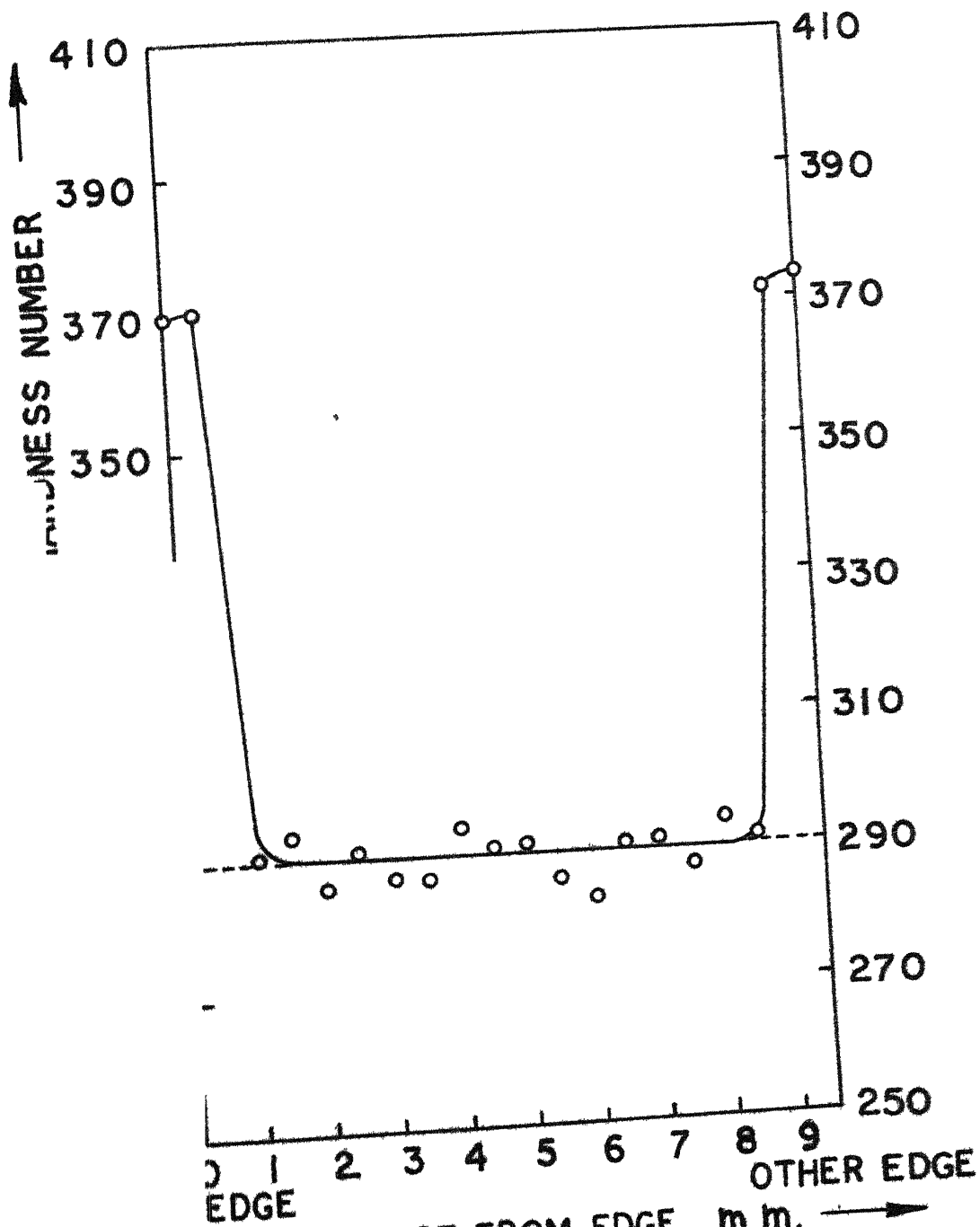


FIG.30. MICROHARDNESS OF Zr-2.5 Nb-4V LEVI-TATION MELTED IN AS CAST CONDITION.



II. MICROHARDNESS OF Zr-2.5Nb-1Ti
LEVITATION MELTED IN AS CAST
CONDITION.

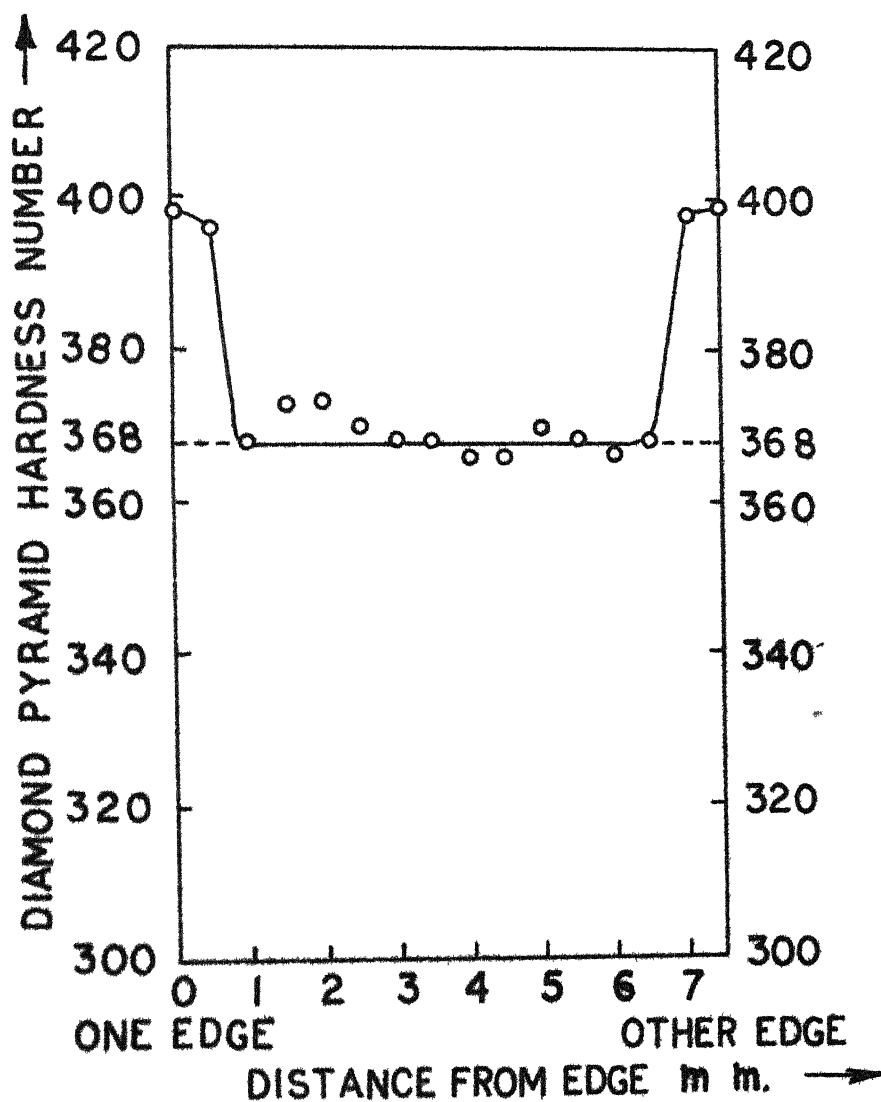


FIG. 32. MICROHARDNESS OF Zr-2.5Nb
-2Ti LEVITATION MELTED IN AS
CAST CONDITION.

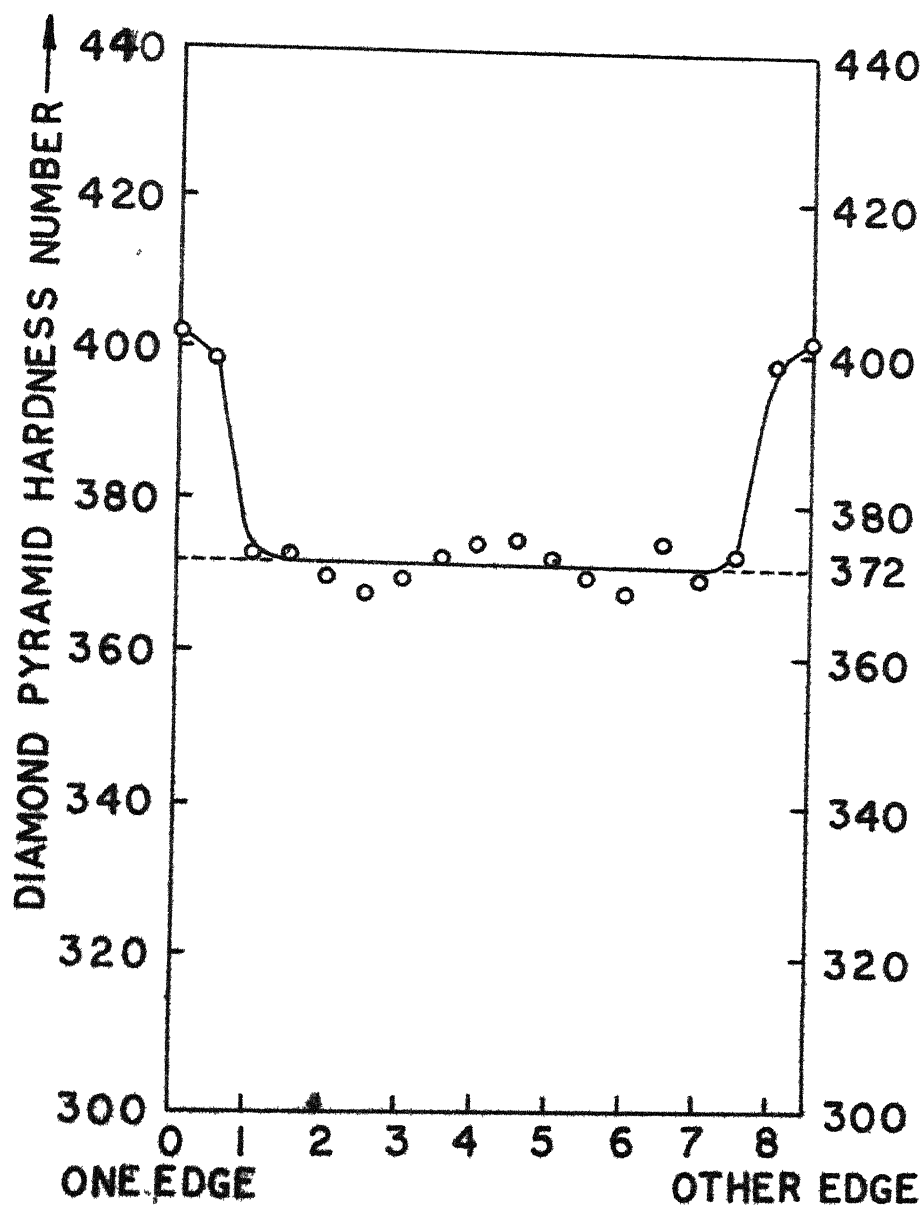


FIG.33. MICROHARDNESS OF Zr-2.5Nb-3Ti
LEVITATION MELTED IN AS CAST
CONDITION.

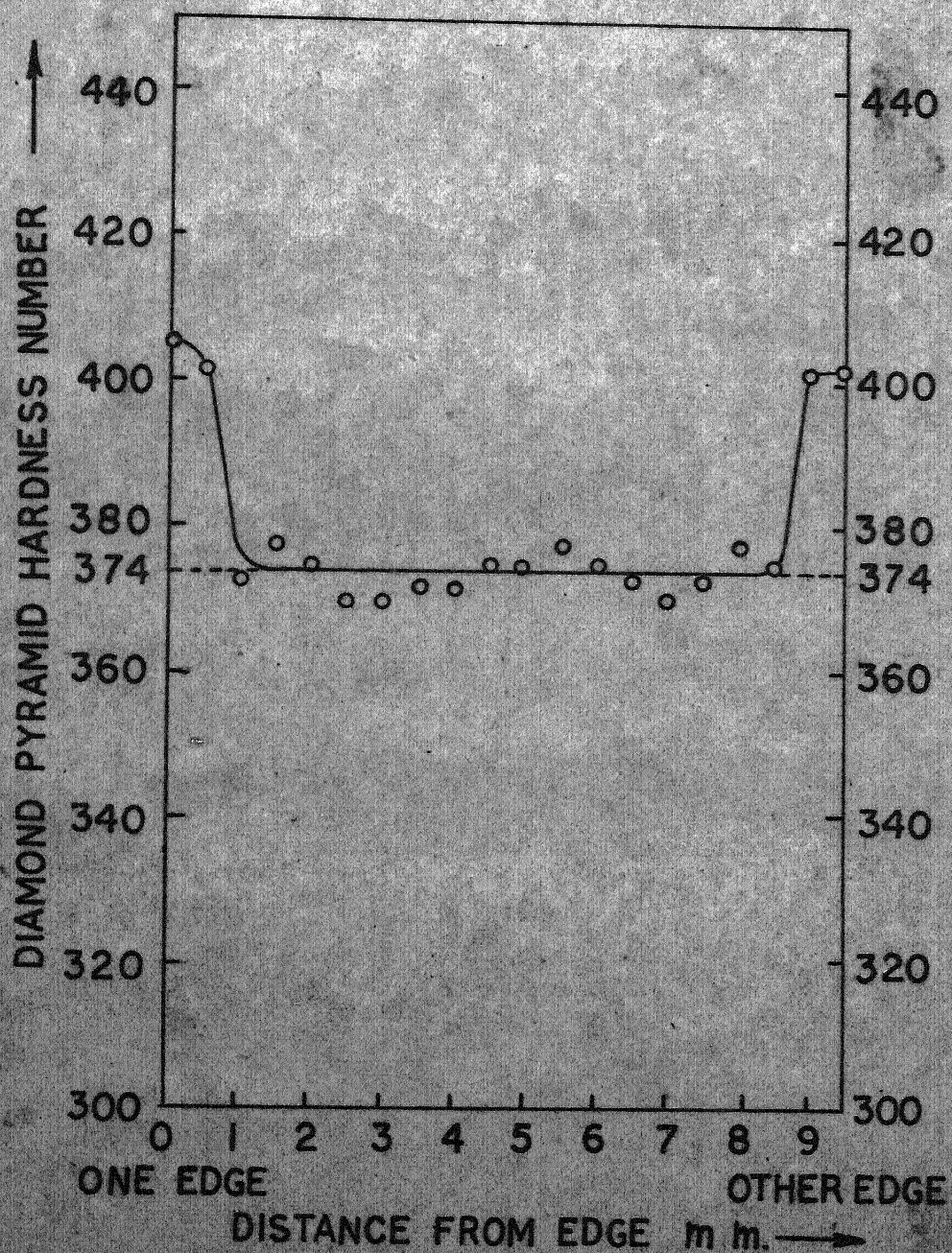


FIG.34. MICROHARDNESS OF Zr-2.5Nb-4Ti
LEVITATION MELTED IN AS CAST
CONDITION.

CHAPTER - VI

DISCUSSION

The levitation coil as described on page 19 for successful levitation of Zirconium and Zirconium-Niobium alloys was developed. With the help of such coil it was possible to make several alloys of Zr-Nb and Zr-Nb with minute additions of Titanium and Vanadium. This achievement is significant in the light that several attempts of Wroughton et al²⁸ (1952) to levitate molten Zirconium in a vacuum failed; though they could successfully levitate melt Al, Sn and Brass. However, in 1958 Comenetz³⁹ could levitate melt Zirconium and its alloys. During the present investigations when it was tried to levitate Zirconium with the coil described by Comenetz³⁸, little success was obtained. Such a failure is difficult to explain. Perhaps proper matching of the load (Zirconium) with the coil suggested by Comenetz³⁸ could not be obtained. After many trials and errors it was possible to arrive at coil design which could successfully levitate melt Zirconium and its alloys. This coil was conical in shape similar to one described by Comenetz³⁸ but differed in coil semiapex angle, in present case the angle being 30° and also in distance between two turns of the coil, in present case distance being 1/12". When this distance between two coils was reduced to less than 1/12", a lot of sparking

between the coil turns was observed especially at higher voltage. When the distance was made larger than , there was not found sufficient levitation force and the metal or alloy invariably stuck with the coil.

Coils with apex semi angle varying from 20 to 60° were tried. But the coil with semi apex angle 30° was found to give best results. Such a coil for successful levitation was arrived at largely by trials and errors. It is since 15 years that first levitation coil was successfully tested by Okress et al²⁷ and since then various articles on the subject appeared, but even today no exact mathematics is available for designing the coil for levitation. Work in the direction of developing mathematics for coil design may help solve the problem of levitating any metal.

With the present coil, the maximum amount that was levitated was 1.5 to 2 gm. However, upto 10 gm. levitation of many metals has been reported by Comenetz³ et al³⁸. All the attempts to levitate melt higher amount than 2 gm. with this coil or other coil failed.

In present case levitation melting was done in inert atmosphere of Argon at 1 atm. pressure. When the melting was tried in vacuum of order of 10 microns, there was heavy sparking between the coils, and no levitation melting occurred. Even at pressure of less than 1 atm. of Argon, there was

sufficient sparking so as to hinder the melting.

Melts repeated under seemingly identical condition did not all succeed. The same statement had been made by Comenetz³⁸ et al of Westinghouse who are pioneers in this field. It shows even today levitation melting remains an art. It appeared that shape and size of the melting charge are very critical and important factors in the levitation. A slight deviation in the shape and size of the charge leads the run to failure. It was observed that for successful levitation charge should be almost cylindrical and of the size such that it just touched the lower most turn of the coil, neither pressing so hard so as to stick to the coil when putting the power on nor so small so as to falling off from the coil during levitation.

During the metallographic examination of Zirconium and Zirconium-Niobium alloys some interesting observations were made. Fig. 5 shows crystal bar Zirconium microstructure. Well defined twins, a characteristic of h.c.p. metal were observed which seemed to have originated from cold working due to grinding and polishing, though sufficient care was taken during specimen preparation.

Microstructure of Zr-2.5 Wt% Nb alloy prepared by levitation melting in the middle of the specimen was identical

to the structure developed by Zr-2.5 Wt% Nb alloy obtained from D.A.E. as seen in Figs. 6 and 7. This structure clearly reveals that Zr-2.5 Wt% Nb is a double phase alloy and not a single phase alloy. This observation contradicts the claims made by Rogers and Akins¹¹, Hodge¹⁴ and Domagala et al¹⁵ who put the solubility limit of Niobium in α -Zirconium to 5% or more. However, more recent and more reliable investigations by Simcoe et al¹³, Richter et al¹⁶, Knapton¹⁸ and Lundin et al¹⁹ who placed solubility limit of Niobium in α -Zirconium less than 0.5 Wt%, 2 Wt%, less than 1 at% and 0.1 Wt% of Niobium respectively, support that Zr-2.5 Wt% Nb alloy is a two phase alloy.

As seen in Fig.8 the micro structure of Zr-2.5 Wt% Nb alloy levitation melted at the edges was of martensitic type. This behaviour was with the expectations as at the edges cooling rate was very high and sufficient to cause β -Zirconium transforming into α' -phase martensitically and is in confirmation with the investigations by Klepper⁴⁷ and Erickson et al⁴⁸ who observed martensite needles in quenched Zirconium upto 5% Niobium alloys.

Figs. 5 - 12 show the microstructure of Zr-2.5 Nb-V alloys. It was noted that these are similar to the structure observed for Zr-2.5 Niobium alloys except that in Zirconium-Niobium-Vanadium alloys martensite needles are thick.

Figs.13 to 20 show the microstructure of Zirconium-Niobium-Titanium alloys. Microstructures of Zr-2.5 Wt% Nb-0.1 Wt% Ti are identical to structures obtained for Zr-2.5 Wt% Nb alloy. Zirconium-Niobium alloys with 0.2 Ti, 0.3 Ti and 0.4 Ti show widmanstätten structure in the centre of the specimen. It appeared that even a small amount of Titanium affects phase transformation in these alloys significantly. Similar structure has been reported by G.S.Slattery⁴⁹ in Zr-2.5 Wt% Nb alloys having acicular needles of transformed ^{Zirconium} with characteristic 90° orientation. Also in Zr-0.19 Wt% O₂ alloy, moderately ^{and} rapidly cooled, Lustman⁵⁰ observed similar widmanstätten structure.

Microhardness testing was carried out with a view to relate structure with the strength. Zr-2.5 Wt% Nb and all the Zr-2.5 Wt% Nb with Vanadium alloys showed D.P.H. values of 286 - 300 in the middle of the specimen as compared to D.P.H. value of 82 of pure Zirconium. It showed that Zirconium can be substantially strengthened by alloying with Niobium. However the addition upto 0.4 of ^V ~~Titanium~~ to Zr-2.5 Wt% Nb alloy did not significantly increase the the strength of the alloy as D.P.H. value of Zr-2.5 Wt% Nb being 286 whereas that of Zr-2.5 Wt% Nb-0.4 Wt% V being 300 D.P.H. only. Microhardness at the edges where martensite needles were observed was very high and remained same to about 371 D.P.H. with and without Vanadium addition. It showed that Zr-2.5 Wt% Nb and

Zr-2.5 Wt% Nb-V alloys can be sufficiently strengthened by heat treatment (quenching).

Microhardness plot of Zr-2.5 Wt% Nb-0.1 Wt% Ti was similar to that for Zr-2.5 Wt% Nb. However, Zr-2.5 Wt% Nb alloys with 0.2 Ti, 0.3 Ti and 0.4 Ti developed very high microhardness of the order of 368 to 374 D.P.H. even in the centre of the specimen where widmanstätten structure was obtained. In these alloys also the microhardness at the edges was higher (of the order of 400 D.P.H.) than that in centre. It can be inferred that addition of small amounts of Titanium increase the strength of Zr-2.5 Wt% Nb alloy substantially. However, the effect of Titanium on other mechanical properties could not be evaluated as specimen size was too small.

X-ray study was also made to determine the phases in the alloys. Powder patterns of crystal bar Zirconium, Zr-2.5 Wt% Nb alloy levitation melted, Zr-2.5 Wt% Nb-0.4 Wt% and Zr-2.5 Wt% Ti alloys were taken. On visual comparison of the powder patterns of alloys with pure Zirconium, no extra lines were observed in any of these alloys. The equilibrium β -Niobium in these alloys expected on the basis of phase diagram by Lundin et al¹⁹ would be 3 Vol. percent. This is about the limit of detection for X-ray diffraction. This finding was in agreement with the observations made by Klepper who could not detect β phase by X-ray examination even in 3 Wt% Nb alloy, though by metallography he got distinct two phase structure in the alloy.

CHAPTER - VII

CONCLUSION

A levitation coil for levitation melting of Zirconium and Zirconium-Niobium alloys is developed. The coil is conical in shape and consists of 7 turns wound in one direction while top turn is wound in reverse direction. It is found that coil with semi apex angle 30° gave the best results. The optimum distance between two coil turns is found to be $1/12"$. The maximum amount of metal that is levitate melted with this coil is 2 gm. Atmosphere in the melting chamber is an important factor for levitation melting. Successful levitation melting occurs in Argon atmosphere at 1 atm. pressure. Melts repeated under seemingly identical conditions do not all succeed. The size and shape of melting charge are very critical and significant factors in the levitation melting. It is observed that melting charge should be almost cylindrical in shape and of the size such that it just touches the bottom most turn of the coil.

During the metallographic examination of the alloys it is observed that Zr-2.5 Wt% Nb alloy is a two phase alloy and thus it is concluded that solubility limit of Niobium in -Zirconium is less than 2.5%. In all the alloys of Zr-2.5 Wt% Nb and Zr-2.5 Wt% Nb-V and Zr-2.5Wt% Nb-Ti at higher cooling

rate martensite needles are obtained. In Zr-2.5 Wt% Nb and Zr-2.5 Wt% Nb-Ti the needles are fine whereas small additions of Vanadium in Zr-2.5 Wt% Nb alloys cause needles to coarsen.

The small additions of Titanium in Zr-2.5 Wt% Nb alloys moderately cooled cause widmanstätten structure to appear. It is thus obvious that Titanium addition affects phase transformation from β to α in Zr-2.5 Wt% Nb alloys significantly.

Microhardness of Zr-2.5 Wt% Nb alloy is considerably higher than that of pure Zirconium. Thus it is concluded that Zirconium can be substantially strengthened by alloying with Niobium. Zr-2.5 Wt% Nb alloy at higher cooling rate when martensite needles are obtained develops higher microhardness than the alloy moderately cooled. This shows the potentiality of Zr-2.5 Wt% Nb alloy to develop higher strength by heat treatment (rapid cooling). Vanadium additions in small amount do not increase microhardness significantly. But small amount of Titanium additions to Zr-2.5 Wt% Nb alloys increase microhardness of the alloys substantially.

However, to decide the suitability of Zr-2.5 Wt% Nb-Ti alloys for fuel element cladding in nuclear reactors, other mechanical tests, eg. ductility and impact testing, and corrosion tests are necessary and more work on these lines is suggested.

Also it may be interesting both from theoretical and practical points of view to study systematically the effects of small additions of other transition metals of 4th and 5th groups on the properties of Zr-2.5 Wt% Nb alloys.

APPENDIX AZIRCALOY -2

Chemical Composition (Wt%)

Sn	1.2 - 1.7	N max	0.010
Fe	0.07 - 0.20	N av	0.008
Cr	0.05 - 0.15	O av	0.170
Ni	0.03 - 0.08		
Zr	Rest		

APPENDIX B

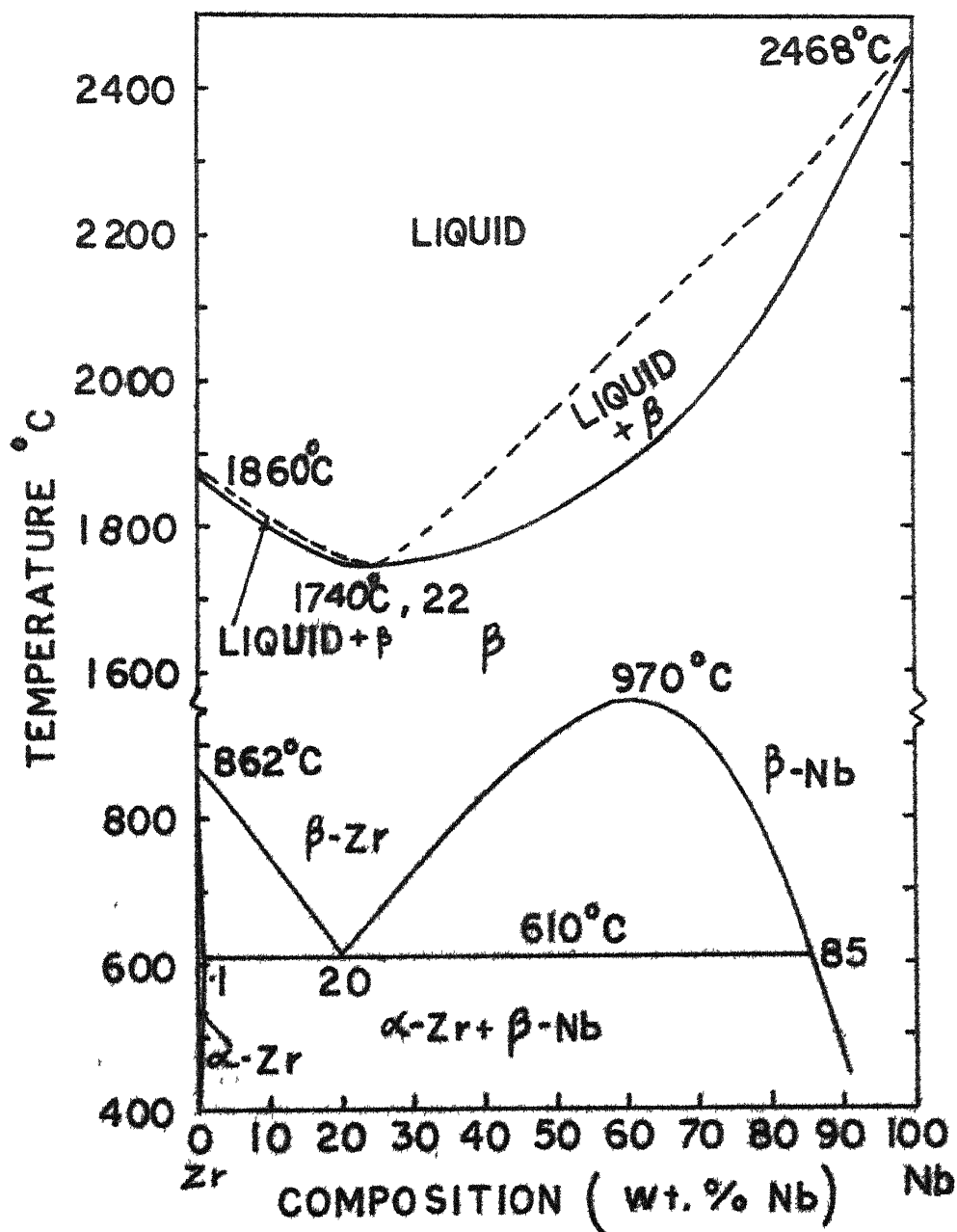


FIG. 35. THE EQUILIBRIUM PHASE DIAGRAM OF Zr-Nb SYSTEM.

REFERENCES

1. G.Fredric, R.Robertson and R.Carpenter
U.S.Bureau of Mines, Report USBM-II-92(1954).
2. R.Arbartsumyan
2nd Geneva Conf. 1958, 15/P/2044.
3. D.L.Douglass, B.Dearing
Knolls Atomic Power Laboratory Schenectady,
N.Y., U.S.A., Report KAPL-2071(1960).
4. S.Dalgard
Chalk river (Canada)
Report CRGM 1030(1961).
5. B.Cox and Coworkers
Harwell U.K. unpublished work.
6. N.Rosler
"Studies in the Corrosion of Zirconium alloys
in superheated steam", Symposium sur la corrosion
dans l', Industrie Nuclaire Paris, Oct.19,1961.
7. K.Anderka and Coworkers
Metal gas cells shaft (Frankfurt),unpublished work.
8. J.K.Dawson, R.C.Asher, B.Watkins, J.Boulton and J.K.Wanklyn
3rd Geneva Conf. 1964 P/158.
9. C.E.Ells, S.B.Dalgard, W.Evans and W.R.Thomas
3rd Geneva Conf. 1964 P/ 22.
10. C.R.Cupp
J.Nuclear Materials, 6, No.3 (1961) pp 241-255.
11. B.A.Roggers and D.F.Atkins
Trans.AIME 203, 1955, pp 1034-1041.
12. S.M.Shelton
U.S.Atomic Energy Comm. Publ.
AF-TR-5932,1949
Also in Met. Astr. 21,1954,869.

13. C.R.Simcoe and W.L.Mudge
U.S.Atomic Energy Comm.Report
WAPD-38(1951).
14. E.S.Hedge
U.S.Atomic Energy Comm.Report
TID-5061 (1952),pp 461-470.
15. R.F.Domagala and D.J.Mcpherson
Trans. AIME, 206 (1956),pp 619-620.
16. H.Richter, P.Wincierz, K.Anderko and U.Zwicker
J. of Less Common Metals 4 (1962) pp 252-265.
17. Y.F.Bichkov, A.N.Rozanor and D.M.Skorov
Atomic Energy-2 (1957), 146, Translated in
J.Nuclear Energy 5, (1957), pp 402-407.
18. A.G.Knapton
J.of less Common Metals-2, (1960), pp 113-124.
19. C.E.Lundin and R.H.Cox
USAE CTID 11919, (1960).
20. A.H. Roberson
"Metallurgy and Fuels" Progress in Nuclear Energy
Series, Editor H.M.Finiston and J.P.Howe.
21. H.A.Saller, R.F.Dickerson and E.L.Foster Jr.
Vacuum Metallurgy Symposium of the Electrothermic
and Metallurgy Division of the Electrothermic
Society, Oct. 1954.
22. W.J.Kroll
Trans.Electrochem. Soc. 78 (1940) 35.
23. O.W.Simmens, C.T.Greenidge and L.W.Eastwood.
Production and arc melting of Titanium
U.S.Off.Naval Research Titanium Symposium,p 77
Washington 1948.
24. G.L.Miller
Zirconium-Metallurgy of the rarer metals
Second Edition 1957.
25. O.Muck
German Patent No.422,004,Oct.30, 1923.
26. W.V.Lovell
U.S.Patent No.2400869, May 28, 1946 and
2566, 221, August 28, 1951.

27. E.C.Okress and D.M.Wroughton, G.Comenetz, P.H.Brace
and J.C.R.Kelly
J.Appl.Physics 23, 545 (1952).
28. D.M.Wroughton, E.C.Okress, P.H.Brace, G.Comenetz
and J.C.R.Kelly
J.Electrochemical Society 99(1952) p 205.
29. E.C.Okress and D.M.Wroughton
Iron Age 170 (1952) p 83.
30. D.H.Pilonis, R.G.Butters and J.G.Parr
Research 7 (1954) p 273.
31. D.H.Pilonis, R.G.Butters and J.G.Parr
Research 7 (1954) pp S10-12.
32. W.Braunbek
Umschau 53 (1953) p 68.
33. O.Winkler
Zeit. Metallkunde 44 (1953) p 333.
34. W.Schiebe
Metall 7 (1953) p 751.
35. Life Magazine, 1952, June 16, p 49.
36. L.R.Weisberg
Rev.Science Instr. 30 (1959) p 135.
37. D.H.Pillonis and J.G.Parr
Trans. Met.Soc. AIME 200 (1954) p 1148.
38. G.Comenetz and J.W.Salatka
J.Electrochem.Soc. 105 (1958) p 673.
39. G.Comenetz and J.W.Salatka
AIME 93rd Annual Meeting, Feb.1964, New York.
40. W.A.Peifer
J.of Metals 17 (1965) p.487.
41. A.E.Jenkins, B.Harris and L.Baker
Symposium on Metallurgy at High Pressure
and Temperatures, pp 23-43, Met.Soc.AIME
Conference, Vol.22, Gordon and Breach Science
Publication, New York, 1964.

42. F.M.Caine
Symposium Amer.Soc.Metals Zirconium and
Zirconium alloys, 1953, pp 533-535.
43. P.A.Jaiquet
Metallurgia 42 (1950) pp 530-533.
44. B.W.Mott and H.R.Hainess
J.Inst.Met. 80 (1952) pp 531-533.
45. A.H.Roberson
Metal Progr. 57 (1949) p 667.
46. H.P.Roth
Metal Progr. 58 (1950) p 709
47. H.H.Khepper
J.of Nuclear Materials 9, No.1 (1963) p 65.
48. W.H.Erickson and D.Hardie
J.of Nuclear Materials 11, No.3 (1964)p 341.
49. G.S.Slattery
J.of Less Common Metals 8 (1965) pp 193-208.
50. B.Lustman
The Metallurgy of Zirconium, p 360,
McGraw-Hill Book Co. Inc., 1955.

© 2004 Blackwell Publishing Ltd *Journal of Internal Medicine* 255: 103–110

[illegible]

—